Hydrogen Oxidation

DOI: 10.1002/ange.201410951

Chemical-Reaction-Induced Hot Electron Flows on Platinum Colloid Nanoparticles under Hydrogen Oxidation: Impact of Nanoparticle Size**

Hyosun Lee, Ievgen I. Nedrygailov, Changhwan Lee, Gabor A. Somorjai,* and Jeong Young Park*

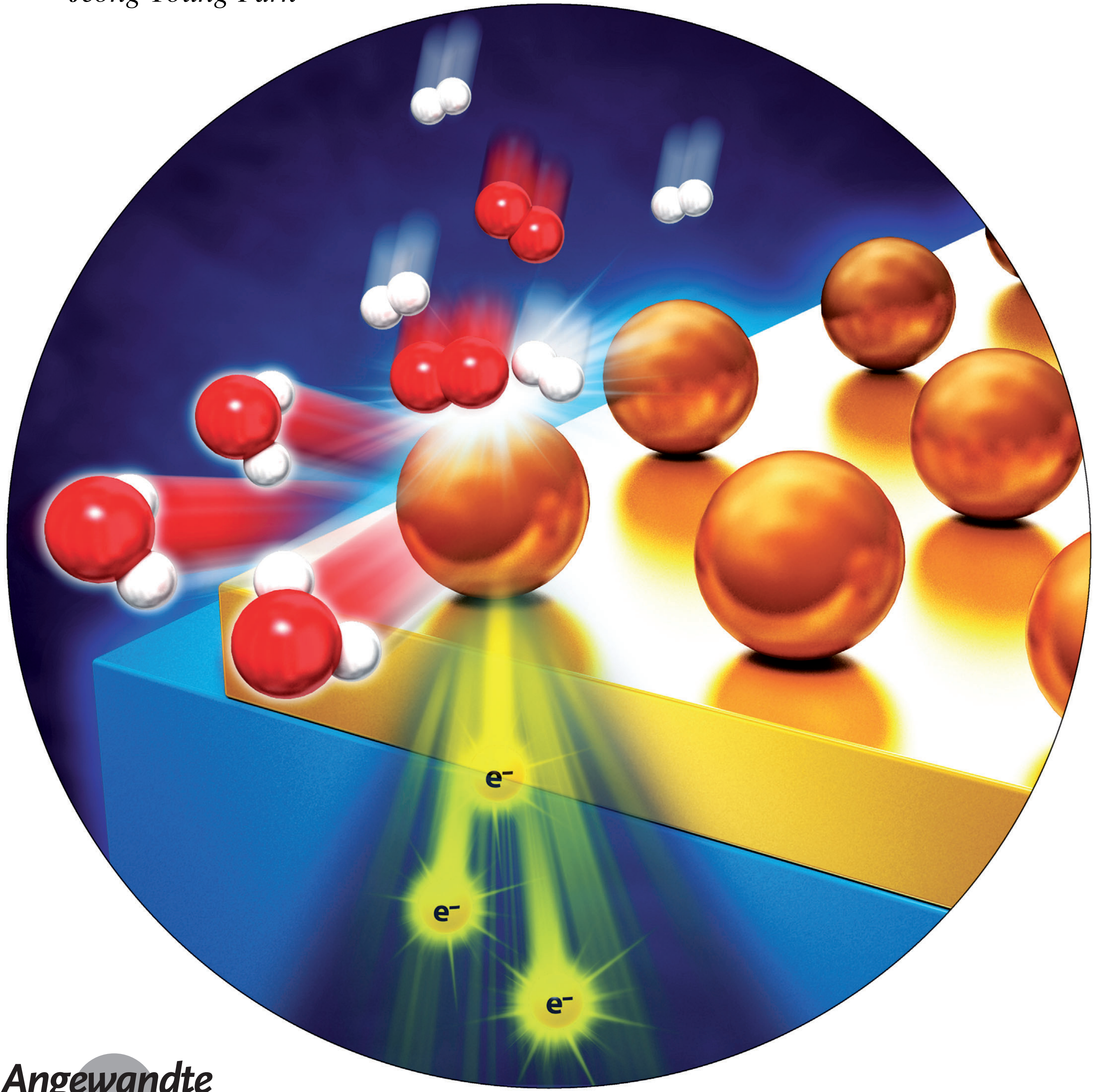

Abstract: *Generation of hot electron flows and the catalytic activity of Pt nanoparticles (NPs) with different sizes were investigated using catalytic nanodiodes. We show that smaller Pt NPs lead to higher chemicurrent yield, which is associated with the shorter travel length for the hot electrons, compared with their inelastic mean free path. We also show the impact of capping on charge carrier transfer between Pt NPs and their support.*

Understanding the fundamental aspects of energy dissipation at surfaces and interfaces is essential for further development of heterogeneous catalysis and environmentally friendly technologies for energy conversion.[1] Once the excess energy of an exothermic chemical reaction is released on the surface, the dissipation process is mediated by the excitation of nuclear and electronic degrees of freedom.[2] The role of the latter process is not yet entirely clear, in spite of the recent development of experimental methods that allow the detection of chemically excited charge carriers. In the pioneering work of McFarland and co-workers, the generation of hot electrons during adsorption of hydrogen atoms on a metal surface was observed using thin-film metal–semiconductor diodes.[3] Later, various Schottky diodes were suggested as model systems for detecting hot electrons generated in the steps of surface reactions.[2a,4] The term catalytic nanodiode has been proposed to denote such thin-film Schottky structures for detection of hot electron flows under catalytic reactions.

Despite the progress in experimental methods for direct detection of chemically excited hot electrons, achieved through the creation of catalytic nanodiodes, investigation of charge transfer associated with the dissipation of chemical energy on metal nanoparticles (NPs) remains challenging. Currently, catalysts composed of supported metal NPs are considered to be the most promising systems for creating advanced catalysts with enhanced activity and selectivity.[5] Among other characteristics, metal NPs synthesized by colloidal methods have gained significant attention because of their well-defined surface structure.[6] Recent studies have demonstrated that the size of colloidal NPs is responsible for significant changes in catalytic performance.[7] Furthermore, changes in catalytic activity occur mostly for nanoparticles 1–10 nm in size.[1]

To extend the applicability of catalytic nanodiodes to the study of energy dissipation mediated by hot electrons during chemical reactions on metal NPs, a new approach has been recently discussed.[4b] In particular, catalytic metal NPs can be deposited as two-dimensional arrays on the chemically inert surface of Schottky nanodiodes, allowing the observation of hot electrons generated on the NPs under dynamic reactions. Studies of this kind are of great importance as they can lead to an understanding of the catalytic properties of the NP catalysts. Herein, we report the processes of hot electron creation and transport in Pt NPs during H_2 oxidation. To allow the detection of chemically excited hot electrons, 1.7 or 4.5 nm Pt NPs (Figure S1 in the Supporting Information) were deposited onto the surface of Au/TiO_2 nanodiodes. A schematic view and energy band diagram of the fabricated Au/TiO_2 nanodiodes with Pt NPs are shown in Figure 1 a and 1 b, respectively. Current–voltage (*I*–*V*) curves of the nanodiodes were recorded (Figure S2) and a Schottky barrier of 0.97 eV was obtained by fitting the data to the thermionic emission equation.[8] Thermal stability of the system also was guaranteed by the electrical and morphological properties (Figures S3 and S4). Further details of the fabrication and characterization of the Au/TiO_2 nanodiodes with Pt NPs are given in the Supporting Information.

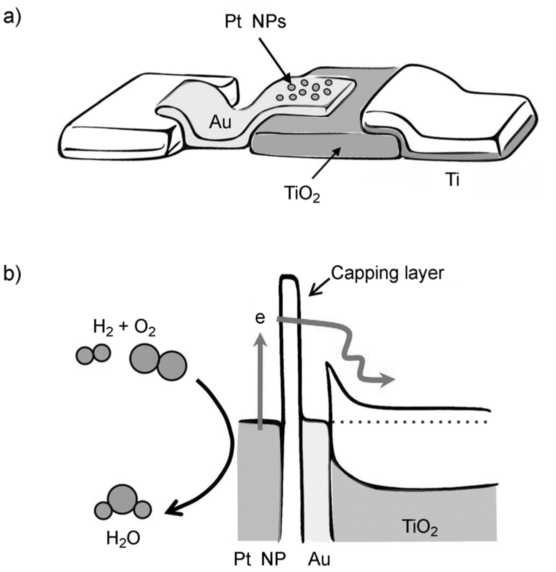

Figure 1. a) Cross-sectional schematic of the Au/TiO_2 nanodiodes with Pt NPs. b) Energy band diagram for Au/TiO_2 nanodiodes with Pt NPs. Hot electrons excited by H_2 oxidation on the Pt NPs must travel through the capping layer before entering the Au/TiO_2 nanodiode where they can be detected.

Figure 2 a, b shows the temperature dependence of the current, measured on the Au/TiO_2 nanodiodes with Pt NPs, in the H_2 (15 Torr) + O_2 (745 Torr) mixture when H_2 oxidation takes place. The conductive properties of the Au/TiO_2 nanodiodes could change during the catalytic reaction as

---

[*] H. Lee, I. I. Nedrygailov, C. Lee, Prof. J. Y. Park
Center for Nanomaterials and Chemical Reactions
Institute for Basic Science
Daejeon 305-701 (Korea)
and
Graduate School of EEWS
Korea Advanced Institute of Science and Technology (KAIST)
Daejeon, 305-701 (Korea)
E-mail: jeongypark@kaist.ac.kr
Prof. G. A. Somorjai
Department of Chemistry, University of California, Berkeley
CA 94720 (USA)
E-mail: somorjai@berkeley.edu

[**] The work was supported by IBS-R004-G4, Republic of Korea, and by the Director, Office of Science, Office of Basic Energy Sciences, Division of Chemical Science, Geological and Biosciences of the US Department of Energy under contract DE-AC02-05CH11231.

Supporting information for this article is available on the WWW under http://dx.doi.org/10.1002/anie.201410951.

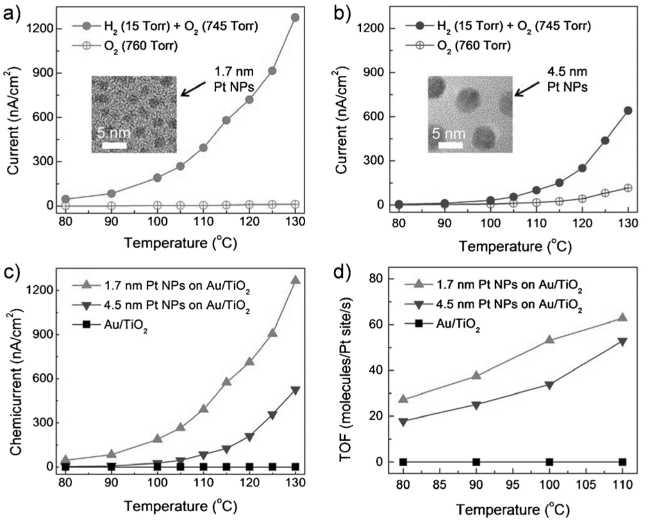

Figure 2. The temperature dependence of the current measured on the Au/TiO$_2$ nanodiodes with a) 1.7 nm or b) 4.5 nm Pt NPs in the H_2+O_2 mixture and in pure O$_2$. The insets show TEM images of the Pt NPs. c) The chemicurrent associated with the H$_2$ oxidation reaction. The current measured from the Au/TiO$_2$ nanodiodes without Pt NPs is also shown for comparison. d) Catalytic activity for H$_2$ oxidation, measured at different temperatures on Au/TiO$_2$ nanodiodes with and without Pt NPs.

a result of heating. In particular, the Schottky barrier height decreases at elevated temperature, which may change the sensitivity of the nanodiode. To exclude this effect, additional current measurements were carried out in pure O$_2$ (760 Torr; Figure 2a,b). Furthermore, the current associated with H$_2$ oxidation was found to be the difference between the currents measured in the H_2+O_2 mixture and in pure O$_2$. Hereafter, this current is denoted as the chemicurrent.

Figure 2c shows the chemicurrent as a function of temperature, measured on the Au/TiO$_2$ nanodiodes with 1.7 or 4.5 nm Pt NPs. For comparison, the current measured on the Au/TiO$_2$ nanodiode without Pt NPs is also shown. The chemicurrent measured on the Au/TiO$_2$ nanodiodes with Pt NPs shows a clear tendency to rise with temperature. The strongest chemicurrent is measured on the nanodiodes decorated with 1.7 nm Pt NPs. This current is notably greater than the chemicurrent measured on the nanodiodes with 4.5 nm Pt NPs over the entire temperature range. At the same time, the current measured on the Au/TiO$_2$ nanodiodes without Pt NPs is close to zero throughout the whole temperature range. All of the currents shown in Figure 2 are normalized with respect to the coverage of Pt NPs on the surface of the Au thin film and presented as a current density (nA cm^{-2}). The SEM images shown in Figure S1 were used to calculate the coverage of the Pt NPs. Additionally, we fabricated Au/TiO$_2$ nanodiodes with 30 nm thick Au electrodes, deposited 1.7 and 4.5 nm Pt NPs on the Au surface, and found that the chemicurrent drops almost to zero when the thickness of the Au film increases in both cases (Figure S5). This result indicates that the chemicurrent is due to the transport of hot electrons excited on Pt NPs in the H$_2$ oxidation reaction.

The trend demonstrated by the chemicurrent in Figure 2c correlates well with the temperature dependence of turnover frequency (TOF) measured for 1.7 and 4.5 nm Pt NPs deposited on a SiO$_2$ substrate (Figure 2d). In addition, it shows the TOF measured on a 10 nm thick continuous Au film, which was fabricated the same way as the top electrode of the Au/TiO$_2$ nanodiodes.

Figure 3 shows Arrhenius plots obtained from measurements of a) TOF and b) chemicurrent detected by the Au/TiO$_2$ nanodiodes with 1.7 or 4.5 nm Pt NPs. For comparison, the data obtained from the Au/TiO$_2$ nanodiodes with the surface covered by a 4 nm thick continuous Pt film are also shown in Figure 3. The activation energy (E_a) for H$_2$ oxidation on the Pt NPs and on the Pt film was estimated from the slope of the Arrhenius plots. According to the TOF measurements, the 1.7 and 4.5 nm Pt NPs and the Pt film show similar activation energies with the mean value of $E_a=(8.7\pm 0.9)$ kcal mol^{-1}. This value agrees well with the previously reported activation energies obtained for H$_2$ oxidation on platinum.[9] In general, the activation energy for the oxidation of hydrogen on platinum, measured by various methods, is in the range of 2.9–20.1 kcal mol^{-1}.[10]

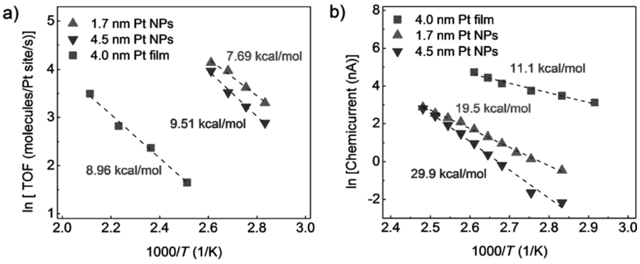

Figure 3. Arrhenius plots obtained from measurement of the a) turnover frequency and b) chemicurrent detected by the Au/TiO$_2$ nanodiodes decorated with 1.7 or 4.5 nm Pt NPs, or a 4 nm thick continuous Pt film.

The activation energy for H$_2$ oxidation, $E_a=(11.1\pm 0.9)$ kcal mol^{-1}, determined using the chemicurrent measured on the Au/TiO$_2$ nanodiodes covered by a 4 nm thick continuous Pt film, is close to the value obtained from the TOF measurements. At the same time, values obtained from measuring the chemicurrent with 1.7 or 4.5 nm Pt NPs are significantly higher ($E_a=(19.5\pm 0.9)$ kcal mol^{-1} for 1.7 nm Pt NPs; $E_a=(29.9\pm 0.9)$ kcal mol^{-1} for 4.5 nm Pt NPs).

To elucidate the reasons for such a large difference between the activation energy obtained from the TOF and chemicurrent measurements, we estimated a chemicurrent yield for each case. As previously shown,[2a,4c,11] the chemicurrent is proportional to the reaction rate. Thus, we can express the dependence of the chemicurrent measured on the Au/TiO$_2$ nanodiodes on the TOF during H$_2$ oxidation according to Equation (1):

$$I = \alpha q A N_{\mathrm{Pt}} \mathrm{TOF} \qquad (1)$$

where α is the chemicurrent yield (i.e., the number of hot electrons detected per molecule of product formed on the nanodiode surface), q is the elementary charge, A is the active area of the catalyst, and N_{Pt} is the number of Pt sites per square millimeter. The chemicurrent yield can be found by fitting the measured current of hot electrons, plotted as a function of the TOF, to Equation (1). For the case of the 4 nm Pt nanofilm deposited on the Au/TiO_2 nanodiode, the chemicurrent plotted versus the TOF is a straight line, which gives $\alpha = 3 \times 10^{-4}$ (Figure 4a). This value is in good agreement with estimates made in similar experiments by other investigators.[2a,4b,9,11] At the same time, for Au/TiO_2 nanodiodes with Pt NPs, the chemicurrent as a function of TOF differs substantially from the straight line (Figure 4b,c). We found that such dependence can be fitted to Equation (1) by taking the chemicurrent yield as a temperature-dependent function, similar to those described by the Arrhenius equation [Equation (2)]:

$$\alpha = \alpha_0 \exp\left(-\frac{\Phi}{k_{\mathrm{B}} T}\right) \tag{2}$$

where Φ is a parameter similar in meaning to the activation energy in the Arrhenius equation. Fitting the chemicurrent measured on the Au/TiO_2 nanodiodes with Pt NPs to Equation (1), in which the chemicurrent yield calculated according to Equation (2) is substituted, gives $\Phi = 8.42$ kcal mol^{-1} and $\Phi = 9.34$ kcal mol^{-1} for the 1.7 and 4.5 nm Pt NPs, respectively. These values allow one to explain the difference in activation energy on the basis of the chemicurrent and TOF measurements, as shown in Figure 3. Further details are given in the Supporting Information. In addition, the value of the chemicurrent yield varies with the Pt NPs size, which is clearly seen in Figure 4d.

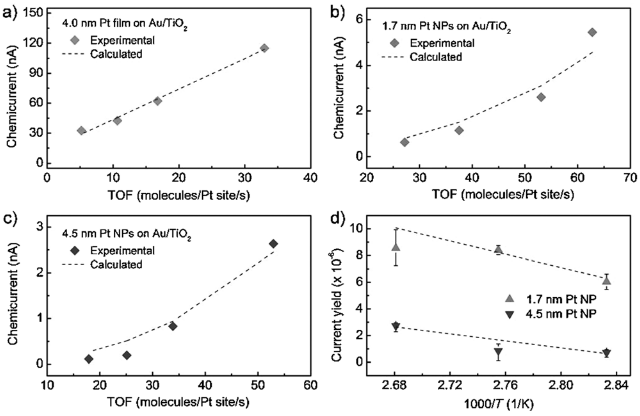

Figure 4. Chemicurrent from the Au/TiO_2 nanodiodes with a) 4 nm thick continuous Pt film, b) 1.7, or c) 4.5 nm Pt NPs, plotted as a function of the TOF for H_2 oxidation. d) Comparison of chemicurrent yield during reaction with 1.7 or 4.5 nm Pt NPs.

Interestingly, experiments conducted under similar conditions using Pt/TiO_2 nanodiodes gave equal values for the activation energy,[12] which are similar to results obtained in the present work. Therefore, following the reasoning set out in reference [4b], we attribute the difference in activation energy for Au/TiO_2 nanodiodes with Pt NPs or a continuous Pt film to charge-transport peculiarities through the capping layer that exists between the Pt NPs and the Au surface. This can be due to a) charging of the capping agent as a result of trapped hot electrons, or b) the potential barrier created by the capping layer because of a Coulomb blockage induced by hot electrons reflected back from the Pt NPs/capping layer interface.[4b] Both mechanisms would lead to a temperature-dependent chemicurrent yield. However, the physical meaning of the parameter Φ would be different. In the case of mechanism (a), Φ would give the depth of electrons in the capping layer, while in mechanism (b) Φ would be the height of the potential barrier formed by the capping layer.

Mechanisms for the electric conductance of capping agents based on solid polymers, such as PVP, deserve a more thorough investigation, which is beyond the scope of this article. However, studies of the electric properties of PVP films showed an Arrhenius-type relation between the conductivity of PVP and temperature.[13] The activation energy was found to be about 12.2 kcal mol^{-1}, which is on the same order as Φ that was calculated in this article from the chemicurrent. This fact may serve as evidence of the validity of the assumptions about charging of the capping layer as a result of the trapping of electrons. Thus, the temperature-activated conductivity turned out to be a property of the capping agent alone, rather than the Pt NPs/capping layer interface.

In summary, we have presented a study of the effect of hot electrons associated with H_2 oxidation on the surface of 1.7 and 4.5 nm colloidal Pt NPs deposited on Au/TiO_2 nanodiodes. In particular, H_2 oxidation over platinum thin films leads to a flow of hot electrons with an intensity proportional to the reaction rate. The smaller Pt NPs show a catalytic activity three times higher than that of the larger Pt NPs, as is clearly seen from both the chemicurrent and turnover frequency measurements.

Received: November 18, 2014

Keywords: catalytic nanodiodes · hot electrons · hydrogen oxidation · nanoparticles · platinum

---

[1] G. A. Somorjai, J. Y. Park, *Angew. Chem. Int. Ed.* **2008**, *47*, 9212–9228; *Angew. Chem.* **2008**, *120*, 9352–9368.

[2] a) H. Nienhaus, *Surf. Sci. Rep.* **2002**, *45*, 1–78; b) G. A. Somorjai, Y. Li, *Introduction to Surface Chemistry and Catalysis*, Wiley, Hoboken, **2010,** pp. 335–387.

[3] B. Gergen, H. Nienhaus, W. H. Weinberg, E. W. McFarland, *Science* **2001**, *294*, 2521–2523.

[4] a) X. Ji, A. Zuppero, J. M. Gidwani, G. A. Somorjai, *Nano Lett.* **2005**, *5*, 753–756; b) J. Y. Park, H. Lee, J. R. Renzas, Y. Zhang, G. A. Somorjai, *Nano Lett.* **2008**, *8*, 2388–2392; c) E. G. Karpov, I. Nedrygailov, *Phys. Rev. B* **2010**, *81*, 205443.

[5] a) S. Tauster, S. Fung, R. Garten, *J. Am. Chem. Soc.* **1978**, *100*, 170–175; b) K. An, S. Alayoglu, N. Musselwhite, K. Na, G. A. Somorjai, *J. Am. Chem. Soc.* **2014**, *136*, 6830–6833.

[6] a) A. Roucoux, J. Schulz, H. Patin, *Chem. Rev.* **2002**, *102*, 3757–3778; b) H. Lee, S. E. Habas, S. Kweskin, D. Butcher, G. A. Somorjai, P. Yang, *Angew. Chem. Int. Ed.* **2006**, *45*, 7824–7828; *Angew. Chem.* **2006**, *118*, 7988–7992; c) G. A. Somorjai, J. Y. Park, *Top. Catal.* **2008**, *49*, 126–135.

[7] a) M. E. Grass, Y. Zhang, D. R. Butcher, J. Y. Park, Y. Li, H. Bluhm, K. M. Bratlie, T. Zhang, G. A. Somorjai, *Angew. Chem. Int. Ed.* **2008**, *47*, 8893 – 8896; *Angew. Chem.* **2008**, *120*, 9025 – 9028; b) R. Narayanan, M. A. El-Sayed, *Nano Lett.* **2004**, *4*, 1343 – 1348; c) S. H. Joo, J. Y. Park, J. R. Renzas, D. R. Butcher, W. Huang, G. A. Somorjai, *Nano Lett.* **2010**, *10*, 2709 – 2713.
[8] S. M. Sze, K. K. Ng, *Physics of semiconductor devices*, Wiley, Hoboken, **2006**, pp. 154 – 162.
[9] A. Hervier, J. R. Renzas, J. Y. Park, G. A. Somorjai, *Nano Lett.* **2009**, *9*, 3930 – 3933.
[10] a) S. Völkening, K. Bedürftig, K. Jacobi, J. Wintterlin, G. Ertl, *Phys. Rev. Lett.* **1999**, *83*, 2672; b) A. B. Anton, D. C. Cadogan, *Surf. Sci.* **1990**, *239*, L548 – L560; c) J. N. Smith Jr, R. L. Palmer, *J. Chem. Phys.* **1972**, *56*, 13 – 20.
[11] E. Karpov, I. Nedrygailov, *Appl. Phys. Lett.* **2009**, *94*, 214101.
[12] J. Y. Park, G. A. Somorjai, *ChemPhysChem* **2006**, *7*, 1409 – 1413.
[13] M. Ravi, Y. Pavani, K. Kiran Kumar, S. Bhavani, A. Sharma, V. Narasimha Rao, *Mater. Chem. Phys.* **2011**, *130*, 442 – 448.